

RSC Advances



This is an *Accepted Manuscript*, which has been through the Royal Society of Chemistry peer review process and has been accepted for publication.

Accepted Manuscripts are published online shortly after acceptance, before technical editing, formatting and proof reading. Using this free service, authors can make their results available to the community, in citable form, before we publish the edited article. This *Accepted Manuscript* will be replaced by the edited, formatted and paginated article as soon as this is available.

You can find more information about *Accepted Manuscripts* in the [Information for Authors](#).

Please note that technical editing may introduce minor changes to the text and/or graphics, which may alter content. The journal's standard [Terms & Conditions](#) and the [Ethical guidelines](#) still apply. In no event shall the Royal Society of Chemistry be held responsible for any errors or omissions in this *Accepted Manuscript* or any consequences arising from the use of any information it contains.



Journal Name

ARTICLE

Potential hepatoprotective effects of fullereneol nanoparticles on alcohol-induced oxidative stress by ROS

Y. Li,^a H. B. Luo,^b H. Y. Zhang,^c Q. Guo,^c H. C. Yao,^c J. Q. Li,^c Q. Chang,^d J. G. Yang,^b F. Wang,^b C. D. Wang,^e X. Yang,^c Z. G. Liu^{††a} and X. Ye,^{†b}

Received 00th January 20xx,
Accepted 00th January 20xx

DOI: 10.1039/x0xx00000x

www.rsc.org/

The free radical scavenging ability of fullereneols is their most exploited property in biomedical studies. The antioxidant properties and associated mechanisms of fullereneol have been previously investigated, but less research has been done to examine the hepatoprotective effects of fullereneol nanoparticles on alcohol-induced oxidative stress. This study examined the antioxidant effects in rat liver primary hepatocyte exposure to fullereneols dissolved in ethanol. In this study, liver primary hepatocytes of Wistar rats were divided into nine experimental groups that were exposed to ethanol (0.1, 1.0 and 10%), fullereneol dissolved in ethanol (0.1, 1.0 and 10%) and controls (PBS; PBS+fullereneol; Vitamin C (Vc) in 10% ethanol). Results demonstrated that fullereneol nanoparticles in 400 μmol/L exhibited excellent ROS scavenging abilities. This contributed to the anti-inflammatory effects involving reduced alcoholic oxidative damage and the regulated promotion of tumor necrosis factor. The intracorporeal metabolism of rat-intake fullereneol was also evaluated by examining precision-cut rat slices of liver and kidney. All results demonstrated the potential hepatoprotective effects of fullereneol nanoparticles in preventive treatment of alcoholic hepatopathy.

Introduction

Excessive alcohol consumption (EAC) is a worldwide problem that is associated with a significant increase in the risk of cancer in men¹⁻². It is considered to be a major cause of morbidity and mortality. The liver is the most important metabolic organ due to its relationship to the gastrointestinal tract. The liver is therefore the primary target of alcohol metabolite associated hepatotoxicity. According to the WHO report, liver cancer is estimated to be responsible for 746,000 deaths globally each year³. It is the second most common cause of cancer deaths in the world. Alcoholic liver injury is one of the major causes of liver cancer. Alcoholic fatty liver (AFL) is an initial symptom of alcoholic hepatitis caused by

excessive, chronic alcohol consumption⁴. AFL can further develop into alcoholic hepatitis⁵, hepatic fibrosis⁶ and hepatocirrhosis⁷. If left untreated these conditions may develop into liver cancer.

Many experimental and clinical studies have already reported that alcohol induced oxidative damage contributes to liver injury⁸⁻⁹. Reactive oxygen species (ROS) play a key role in this hepatotoxicity mechanism¹⁰. Acute and chronic ethanol treatments have been shown to increase the production of ROS, lower cellular antioxidant levels, and enhance peroxidation in many tissues, especially in the liver¹¹. The inflammation is associated with peroxidation of lipids, protein and DNA¹². ROS mediates the classic pathway from oxidative damage to pathogenesis. Over-expressed ROS destroy the innate antioxidant systems which comprise antioxidants such as glutathione (GSH), vitamins C and E as well as small molecules¹³. The generated product of lipid oxidation, malonaldehyde (MDA), could result in further damage to the DNA¹⁴ and trigger the expression of tumor necrosis factor (TNF)¹⁵. TNF is an important cytokine that regulates the internal inflammatory process. Chronic inflammation is associated with a high cancer risk¹⁶, therefore, endosomal ROS clearance is regarded as one of the most effective ways of protecting the liver from pathological changes and cancer.

Fullerenes have attracted considerable attention in the biomedical field since their discovery in 1985¹⁷. The fullerene family, and especially C60, have potential as biological antioxidants. The antioxidant property is based on the fact that fullerenes possess a large number of conjugated double bonds and the low lying lowest unoccupied molecular orbital (LUMO)

^aSchool of Biology and Pharmaceutical Engineering, Wuhan Polytechnic University, Wuhan 430023, P. R. China.

^bLiquor Marking Biological Technology and Application of Key Laboratory of Sichuan Province, College of Bioengineering, Sichuan University of Science & Engineering, Zigong 643000, P. R. China.

^cSection of Environmental Biomedicine, Hubei Key Laboratory of Genetic Regulation and Integrative Biology, College of Life Sciences, Central China Normal University, Wuhan 430079, P. R. China.

^dDepartment of Chemical and Biomolecular Engineering, Hong Kong University of Science and Technology, Hong Kong Special Administrative Region.

^eSichuan University of Arts and Science, Dazhou 635000, P. R. China.

[†]Corresponding Author: Xin Ye, College of Bioengineering, Sichuan University of Science & Engineering, Zigong 643000, P. R. China. Fax: +86-813-5505872; Tel: +86-18398707596; Email: tornadoxin@163.com.

^{††}Corresponding Author: Zhiguo Liu, School of Biology and Pharmaceutical Engineering, Wuhan Polytechnic University, Wuhan 430023, P. R. China. Fax: +86-27-83956793-208; Tel: +86-15327270600; Email: lzg_wpu@163.com;

can easily take up electrons, making an attack of radical species highly possible¹⁸. However, fullerene-C60 in polar solutions exhibit low solubility, which limits their use in the human body¹⁹. In addition, the potential cytotoxicity of fullerene-C60 is also of great concern²⁰. Chemical modification of C60 double bonds is currently an internationally popular method to provide better properties for fullerene derivatives. The 30 double bonds of C60 are potential modification sites for generating new derivatives with particular desired functions. Hydroxylated fullerenes, also known as fullerenols, have attracted a lot of attention as an important class of fullerene derivatives. Previous studies of fullerenols have demonstrated their good water solubility as well as being non-cytotoxic²¹⁻²⁴. Researchers have also reported that fullerenols exhibit powerful antioxidant capabilities making them useful as potential antioxidative agents for biological systems²⁵⁻²⁶. For example, recent *in vitro* and *in vivo* studies have demonstrated that fullereneol C₆₀(OH)₂₄ has a higher antioxidant activity than that of natural antioxidants such as vitamins A, C and E²⁷⁻²⁸. Animal experiments have shown that the liver is the primary organ that absorbs fullereneol. This absorbed fullereneol is then excreted via the digestive tract and the kidneys²⁹. Therefore, fullereneol is quite promising as a liver tissue-protective agent due to its biocompatibility and radical scavenging activity³⁰⁻³¹. Few studies, however, investigate the hepatoprotective effects of fullereneol in alcoholic liver injury.

The rat primary cultured hepatocyte is the most accepted model for hepatotoxicity and hepatopathy studies³²⁻³³. In this study, we examined the hepatoprotective effects of

fullereneol after rat hepatocytes were subjected to ethanol at different concentrations. The US CDC and US NIAAA (National Institute of Alcohol Abuse and Alcoholism) have established levels of human alcohol intake. Using these established levels as a reference, we used ethanol concentrations of 0.1%, 1% and 10% in our study³⁴. Biomarkers of oxidative stress (ROS, MDA, GSH), DNA damage (8-hydroxy-2'-deoxyguanosine, 8-OHdG) and tumor necrosis factor (TNF- α) were examined. The objective was to identify the hepatoprotective effects of fullereneol in preventive treatment of alcohol induced oxidative stress. The intracorporeal metabolism of rat-intake fullereneol was also evaluated by examining precision-cut slices of liver and kidney.

Results and discussion

Physicochemical characteristics of fullereneol

Size distributions of the tested material were measured using atomic force microscopy (AFM) and a scanning electron microscope (SEM). The AFM image shows the size distribution of dispersed fullerenols (Fig. 1B). Grain size in the nanoscale range was also observed (Fig. 1B). The SEM image in the top right corner demonstrates the morphology of a single fullereneol particle (Fig. 1B). The small size of nanoparticles facilitates the absorption of engineering materials across biological barriers or their uptake by cells³⁵⁻³⁶. This capability allows the experimental fullereneol material to migrate across biological barriers and into target organs. The chemical structure of fullereneol was determined using an automatic elemental analyzer, thermogravimetric analysis and ATR-FTIR.

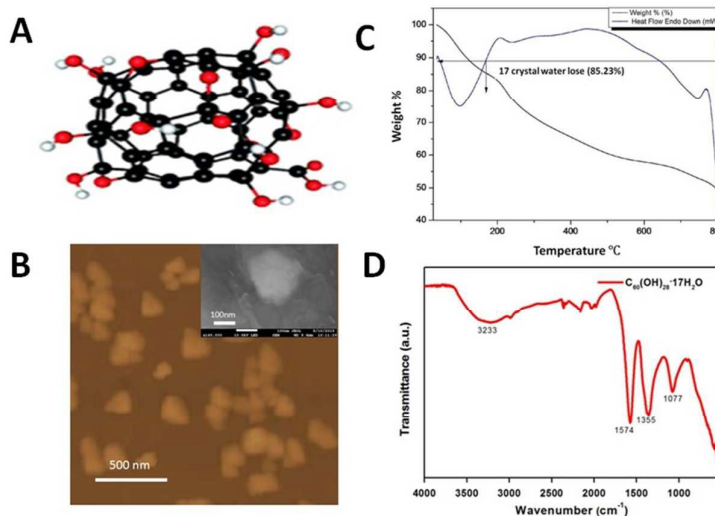


Fig. 1 Characterization of fullereneol. A, Chemical structural formula; B, Images of AFM and SEM; C, Thermal analysis of fullereneol; D, ATR-FTIR spectrum.

The percentages of carbon and of hydrogen in the tested C60 derivative were determined by automatic elemental analyzer, and were found to be 34.855% and 2.955% respectively. 17 molecules of crystallization water loss were also detected by thermal analysis (Fig. 1C). From this analysis we found that the formula of the experimental C60 derivative was $C_{60}(OH)_{28} \cdot 17H_2O$. The FTIR spectrum of the C60 derivative is shown in Fig. 1D. The FTIR spectrum of the C60 derivative contains four sharp absorption peaks at 1077, 1365, 1574, and 3233 cm^{-1} . These peaks are attributed to $\gamma C-O$, $\delta C-O-H$, $\gamma C=C$, and $\gamma O-H$, respectively³⁷. The result of the FTIR analysis is further evidence of a typical fullerene chemical structure of experimental C60. The chemical modification of the fullerene carbon cage by the attachment of functional groups (e.g.-OH) enhances its water solubility via hydrophilic functional adducts. The good solubility of fullerene greatly improves its applicability as a biomedical agent in the human body.

Fullerenol scavenges intracellular ROS induced by ethanol

Ethanol, oxidative stress and associated oxidative damage are mediators of cellular injury in many pathological conditions³⁸⁻³⁹. Both clinical findings and results of experiments with animal models of alcoholic hepatopathy have shown these interactions in the onset of ethanol-induced liver damage³⁹. ROS generation is associated with ethanol stimulation. In the classic ethanol metabolizing pathway, the alcohol dehydrogenase enzyme reacts with the ethanol to form acetaldehyde which is highly unstable and results in the formation of free radicals. The observed intracellular ROS levels seen in this study support this theory.

Acute exposures of ethanol with fullerene to rat liver hepatocytes for 2h were applied in intracellular ROS measurement. ROS generation occurs immediately after ethanol contact with cells. The method of combined exposure is to simulate instantaneous hepatoprotective effects of fullerene in the process of alcohol consumption. Prepared rat liver hepatocytes were initially exposed to different concentrations of ethanol (0.1, 1.0 and 10%) for a 2 h incubation period at 37°C in a CO₂ incubator. Intracellular ROS increased in a dose-dependent manner (Fig. 2A). The ROS increases in all the ethanol groups were extremely significant ($p < 0.001$) as compared to the PBS group. Water-soluble fullerenols have been approved for their antioxidant ability to scavenge oxygen radicals, and for their ability to protect cells and/or tissues against ROS damage⁴⁰. In this test, the average ROS found in the samples containing fullerene nanoparticles in PBS was almost equal to that found in the PBS control. Our results showed that the fullerene nanoparticles had good biocompatibility (Fig. 2A-B). In addition, the fullerene nanoparticles dissolved in ethanol (400 $\mu mol/L$) demonstrated strong scavenging of the ethanol induced ROS (Fig. 2B). The groups with fullerene nanoparticles dispersed in ethanol (0.1% and 1.0%) showed extremely significant differences ($p < 0.001$) when compared to the ethanol only groups (Fig. 2D). ROS averages for the fullerene nanoparticles in ethanol (0.1 and 1.0%) were even closer to the control PBS group. Results demonstrated that fullerene nanoparticles effectively quenched the ROS induced by ethanol (10%). However, it was not as effective with the lower ethanol concentrations of 0.1 and 1% (Fig. 2B). One possible reason is that 10% ethanol induced strong oxidative stress in the rat liver hepatocytes. Fullerene at a higher concentration than

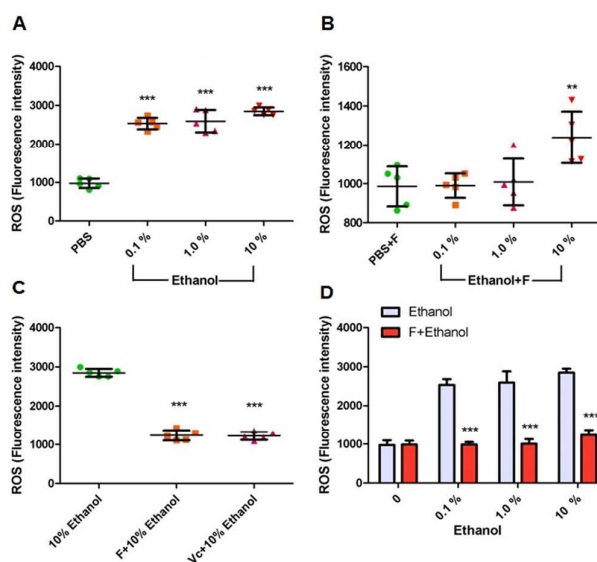


Fig. 2 Fluorescence intensity of intracellular ROS. A, Ethanol with concentration of 0.1, 1.0 and 10%; B, F + Ethanol with concentration of 0.1, 1.0 and 10%; C, The same amount of F and Vc in 10% ethanol; D, Comparison between groups of ethanol and F/Ethanol (F-fullerenol nanoparticles; Vc-Vitamin C; **, $p < 0.01$; ***, $p < 0.001$).

400 $\mu mol/L$ may be better for quenching excessive ROS caused by 10% ethanol. However, as an engineering biomaterial, issues of biocompatibility and metabolism are greatest concern. Further studies of fullerene are needed to ascertain the relationship between "effective dose" and "biocompatible concentration". Fullerene has been approved for its excellent antioxidant properties. Studies have demonstrated its antioxidant activity in *in-vitro* and *in-vivo*, is equal to or higher than that of natural antioxidants such as ascorbic acid (Vitamin C)⁴¹. Similar results have also been seen in prepared rat liver hepatocytes. Average ROS was obviously reduced ($p < 0.001$) in the group where fullerene nanoparticles were dissolved in 10% ethanol. The ROS scavenging efficiency was being equal to that of Vitamin C (Fig. 2C). The fluorescence images of intracellular ROS are shown in Fig. 3A-I.

Covalently attached groups of fullerene might play an important role in ROS scavenging. This specific behavior of fullerenols is due to their structural flexibility, the rotation of the OH- groups around the C-O bond axis, and the distribution of these groups across different carbon sites of the fullerene surface⁴². Based on this flexible structure, several mechanisms behind the antioxidant activity of fullerene nanoparticles have recently been proposed. One such mechanism involves the radical reaction of hydroxyl radicals with the remaining olefinic double bonds of the fullerene core. Fullerene may also function as an antioxidant by donating a hydrogen atom from the hydroxyl group, to the particular radical compound. Another possible mechanism is for the oxygen radical to extract a hydrogen atom or an electron from the fullerene to yield a relatively stable fullerene. The free radicals based on the large numbers of conjugated double bonds with low

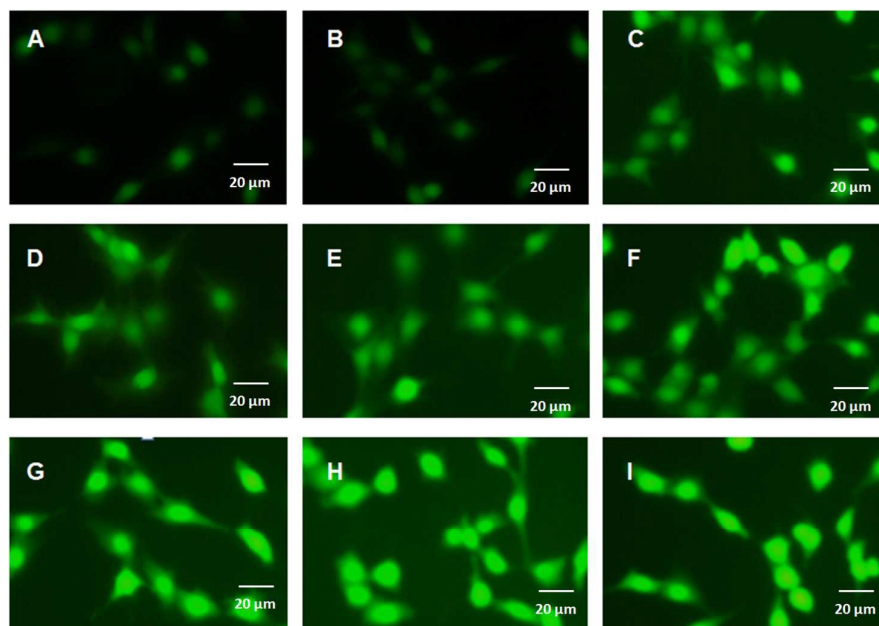


Fig. 3 Fluorescence images of intracellular ROS in liver primary hepatocytes (Nikon, Eclipse TS 100; 40×). A, PBS; B, Fullerenol nanoparticles in PBS; C, Vc in 10% ethanol; D-F, F + Ethanol with concentration of 0.1, 1.0 and 10%; G-I, Ethanol with concentration of 0.1, 1.0 and 10% (F-fullerenol nanoparticles; Vc-Vitamin C).

energy, unoccupied molecular orbitals, can easily take up an electron and facilitate reactions with radical species⁴³⁻⁴⁴.

Hepatoprotective properties of fullerene nanoparticles: resistance to ethanol-induced oxidative damage and inflammation

Ethanol induced oxidative damage in the liver has been demonstrated by experimental data from rats in both acute and chronic tests⁴⁵. In general, cellular antioxidant defences are sufficient to keep the levels of ROS below a toxic threshold. However, toxic agent induced-ROS overproduction could destroy this natural anti-oxidant system⁴⁶. ROS-induced oxidative stress is always determined by measuring levels of biomacromolecules such as malondialdehyde (MDA) and glutathione (GSH). Glutathione (GSH) is an important antioxidant in this system. It is the classical biomarker used to reflect the status of oxidative stress that is indicated by the bioreaction of ROS-oxidized GSH into the oxidized form of glutathione (GSSH).

In this study we found that GSH levels were greatly decreased after liver hepatocytes had been exposed to different concentrations of ethanol. The decrease followed a dose-dependent trend (Fig. 4A). The GSH decrease was significant in the 0.1% ethanol group ($p < 0.01$) and extremely significant in the 1.0 and 10% groups ($p < 0.001$) when compared to the PBS control group. The decrease in GSH levels slowed after fullerenol nanoparticles were added in the ethanol groups (Fig. 4B and D). This protective ability of GSH was equal to that of Vitamin C (Fig. 4C). This is due to the excellent ROS scavenging ability of fullerenol.

Studies have shown that glutathione depletion can induce cell death⁴⁷. Our results for GSH demonstrate that the tested fullerenol nanoparticles can effectively reduce ethanol-associated oxidative stress.

Peroxidation is another consequence of oxidative stress. There is a relationship between lipid peroxidation and ROS production. Both isolated polyunsaturated fatty acids and those incorporated into lipids are easily attacked by free radicals and are oxidized to lipid peroxides⁴⁸. Malondialdehyde (MDA) is a metabolite of the lipid peroxidation of cell membranes. Increased lipid peroxidation is associated with alcohol induced pathological liver injury⁴⁹. Fig. 5A shows that MDA increases were dose dependent according to ethanol concentrations. Fullerenol nanoparticles effectively reduced the generation of MDA (Fig. 5B and Fig 5D). The ability of fullerenol nanoparticles to reduce MDA was similar to that of Vitamin C (Fig. 5C). One possible mechanism to explain this is that tested fullerenol nanoparticles exhibited excellent ROS scavenging ability. In addition, fullerenol nanoparticles have numerous free oxygen electron pairs distributed around the fullerenol surface providing many opportunities to form coordinate bonds with pro-oxidant metal ions⁵⁰. This contributes to the protective abilities of the tested fullerenol nanoparticles against lipid peroxidation.

Excessive activation of oxidative stress can lead to lipid peroxidation which is the leading cause for the expression and genetic mutation of proinflammatory cytokines that may result in cancer⁵¹. For example, oxidative DNA damage is a major source of the mutation load in living organisms. There are

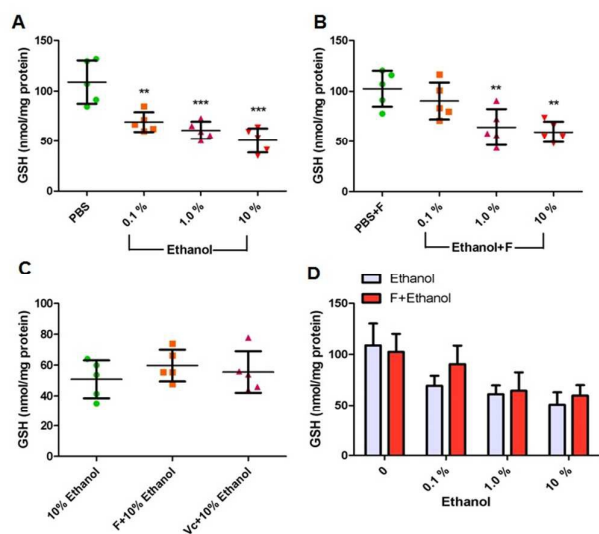


Fig. 4 Intracellular GSH content. A, Ethanol with concentration of 0.1, 1.0 and 10%; B, F + Ethanol with concentration of 0.1, 1.0 and 10%; C, The same amount of F and Vc in 10% ethanol; D, Comparison between groups of ethanol and F/Ethanol (F-fullerenol nanoparticles; Vc-Vitamin C; **, $p < 0.01$; ***, $p < 0.001$).

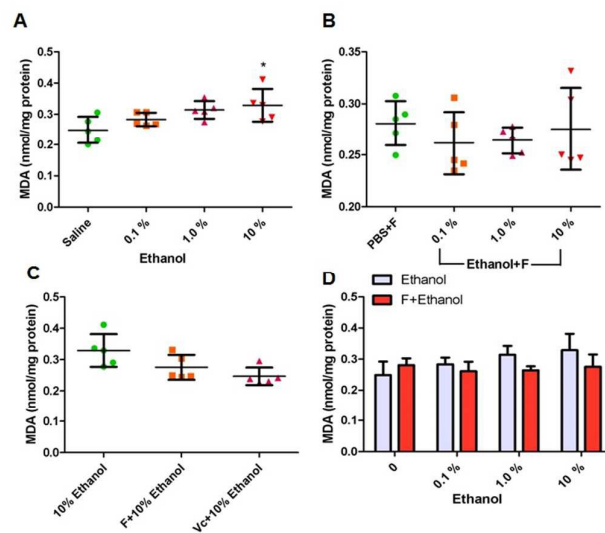


Fig. 5 Intracellular MDA content. A, Ethanol with concentration of 0.1, 1.0 and 10%; B, F + Ethanol with concentration of 0.1, 1.0 and 10%; C, The same amount of F and Vc in 10% ethanol; D, Comparison between groups of ethanol and F/Ethanol (F-fullerenol nanoparticles; Vc-Vitamin C; *, $p < 0.05$).

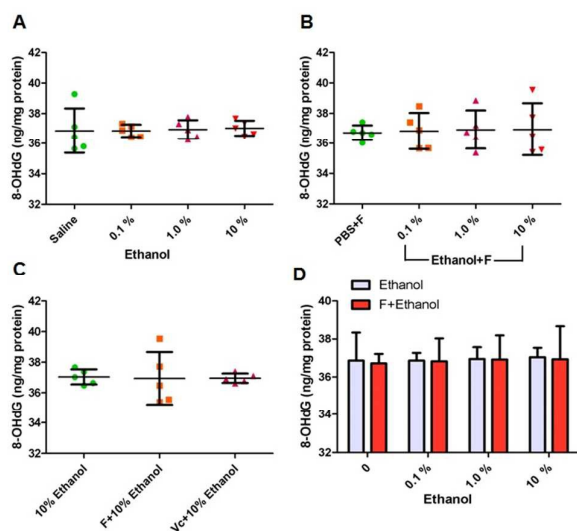


Fig. 6 Intracellular 8-OHdG content. A, Ethanol with concentration of 0.1, 1.0 and 10%; B, F + Ethanol with concentration of 0.1, 1.0 and 10%; C, The same amount of F and Vc in 10% ethanol; D, Comparison between groups of ethanol and F/Ethanol (F-fullerenol nanoparticles; Vc-Vitamin C).

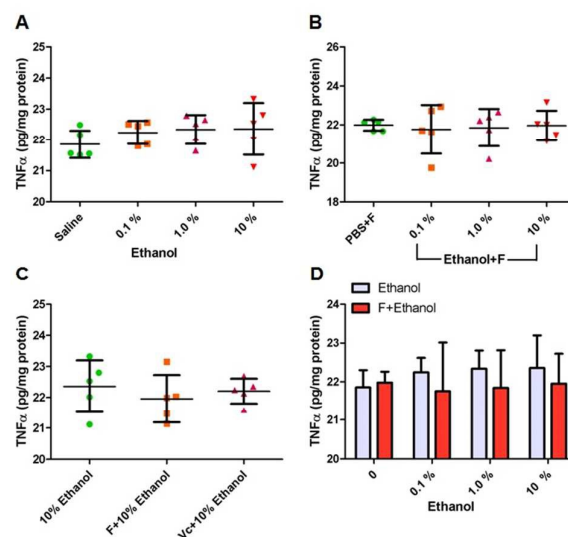


Fig. 7 Intracellular TNF- α content. A, Ethanol with concentration of 0.1, 1.0 and 10%; B, F + Ethanol with concentration of 0.1, 1.0 and 10%; C, The same amount of F and Vc in 10% ethanol; D, Comparison between groups of ethanol and F/Ethanol (F-fullerenol nanoparticles; Vc-Vitamin C).

more than one hundred oxidative DNA adducts identified (e.g. purine, pyrimidine, and the deoxyribose backbone). 8-OHdG is a pro-mutagenic DNA lesion resulting from oxidation damage. In this study, ethanol induced 8-OHdG was measured. No differences were detected in the control, ethanol or fullerene/ethanol groups (Fig. 6A-D). Results indicated that a 2 h ethanol incubation may not induce any DNA damage. However, TNF- α in the liver hepatocytes showed an upward trend after exposure to ethanol (Fig. 7A). TNF- α is a pleiotropic cytokine that induces cellular responses such as proliferation, production of inflammatory mediators, and cell death. TNF- α is involved in pathological processes such as chronic inflammation. Studies have reported that TNF- α is involved in the pathophysiology of the liver. This includes viral hepatitis, alcoholic liver disease and non-alcoholic fatty liver disease⁵²⁻⁵⁴. Other researchers have also demonstrated that TNF- α up expression is associated with promotion and progression of

cancer⁵⁵⁻⁵⁶. As compared to ethanol groups, TNF- α expression was better controlled in the presence of fullerene nanoparticles (Fig. 7B-D). Results clearly demonstrated that tested fullerene nanoparticles exhibit great facility in anti-inflammation. The capabilities of fullerene (ROS scavenging and anti-lipid peroxidation) demonstrated in this study contributed to these results.

Biodistribution and excretion

Nanotechnology and nanomaterials have potential applications in various medical fields, such as diagnostics, imaging, gene and drug delivery and other types of therapy⁵⁷⁻⁵⁸. Recently, much attention has been paid to the bioactive properties of water-soluble fullerenes⁵⁹. In this study, fullerene nanoparticles exhibited a strong hepatoprotective effect. However, the issues of biodistribution and excretion are always of great concern.

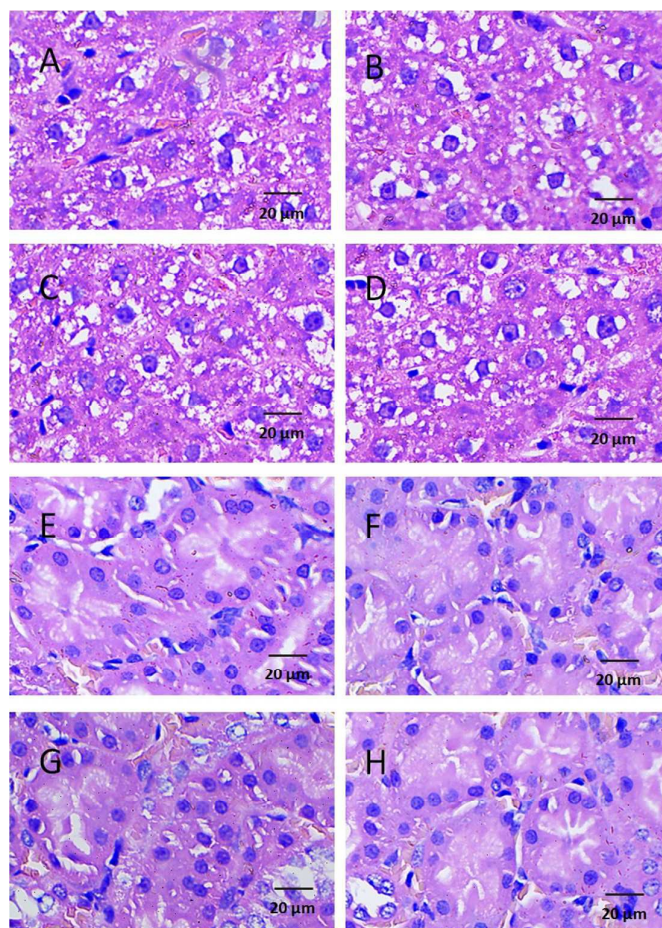


Fig. 8 Biodistribution and excretion of fullerene nanoparticles in metabolic organs of rat. A, PBS-2h (liver); B, PBS-7 day (liver); C, Fullerene-2h (liver); D, Fullerene-7 day (liver); E, PBS-2h (kidney); F, PBS-7 day (kidney); G, Fullerene-2h (kidney); H, Fullerene-7 day (kidney).

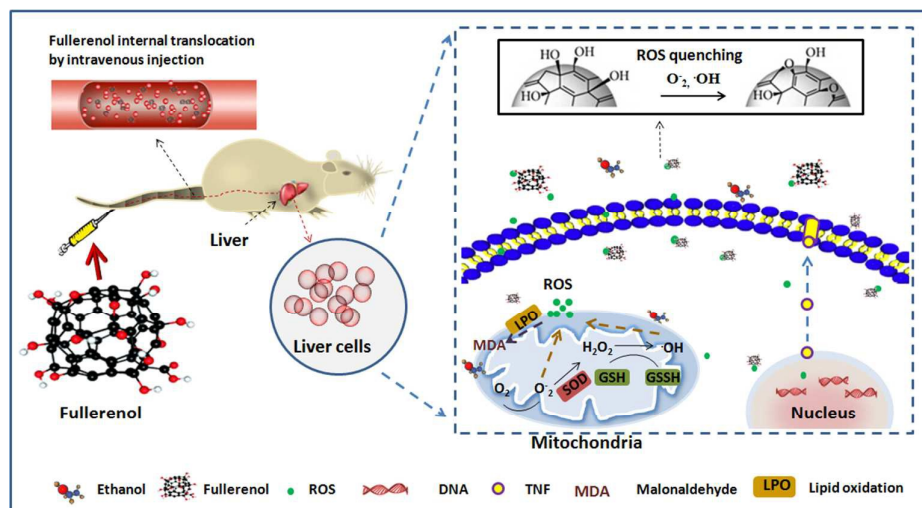


Fig. 9 Mechanism describing the hepatoprotective effect of nano-fullerenol on alcohol-induced hepatotoxicity.

Many studies have reported that fullerenols can effectively distribute and aggregate in the rat liver. The liver is the second most absorptive organ next to the kidney. Ji *et al.* showed via a radiolabeled experiment, the kidney and liver are the main organs that absorb fullerenol⁶⁰. Additionally, results further demonstrated that most fullerenols were excreted from each organ 72 hours after dosing⁶¹⁻⁶². In this study, rats were injected with fullerenol nanoparticles via tail intravenous injection. The two main metabolic organs, the liver and kidney, were studied using H&E-stained tissue slices (Fig. 8). Fine particle clusters were observed in the liver tissue slice (Fig. 8C). The observed results showed that injected fullerenol nanoparticles were successfully transferred to the target organ (the liver) after 2 hours from the time of dose delivery. Issues of biocompatibility and metabolism are of the great concern in preliminary studies of biomedical agents. A correlation study was also carried out using histopathological observations. No pathological inflammatory reactions were observed in the target organs (liver and kidney) after 7 days from the time of dosing (Fig. 8C-D and Fig. 8G-H), when compared to controls (Fig. 8A-B and Fig. 8E-F). Results indicate that fullerenol might be excreted from liver and kidney rather than deposited in these organs. One possible mechanism is that the fullerenol is excreted as metabolized products. Kubota *et al.*⁶³ and Xu *et al.*⁶⁴ independently demonstrated that water-soluble fullerenol could metabolize and be excreted via urine or feces. However, the detailed biodistribution of injected fullerenol nanoparticles *in vivo* is still unknown. An *in vivo* systematic study of metabolism and biological excretion is needed in further studies. In view of all these results, we found that fullerenol nanoparticles play an important role in hepatoprotection from alcohol-induced oxidative stress. In addition, since fullerenol

nanoparticles are a type of biocompatible engineering material, these particles, intravenously injected, could be effectively delivered to the liver (Fig. 9). Liver cell injury is one of the effective models to study alcohol induced oxidative damage and hepatotoxicity. However, liver dysfunction is not limited to liver cell damage, but can also be a function of the internal structure of the organ. For example, a hepatic duct obstruction is a type of non-cytotoxic induced liver disease. A comprehensive study of the hepatoprotective effects of fullerenol still need to be verified by a series of functional hepatic tissue models.

Fullerenol was exhibited potential hepatoprotective effects depend on the existing essays. But the primary limitation of this study is that fullerenol and ethanol were delivered together, whereas the best exposure route would be to first dose the cells with ethanol, followed later by the fullerenol. Sequential dosing should be adopted in future work. It can better simulate the practical conditions of clinical application.

Experimental

Main reagents and kits

Fullerenol ultrafine-particles were purchased from Hengqiu Technologies (Suzhou, Jiangsu, People's Republic of China). Vitamin C was purchased from Sigma-Aldrich (St Louis, MO, USA). The ROS kit was purchased from Merck KGaA (Darmstadt, Germany). Rat ELISA kit for tumor necrosis factor (TNF)- α was purchased from eBioscience (San Diego, CA, USA). Rat enzyme-linked immunosorbent assay (ELISA) kits for 8-OHdG were purchased from Kamiya Biomedical Company (Seattle, WA, USA). Assay kits for MDA, GSH and protein were

purchased from Beyotime (Nanjing, Jiangsu, People's Republic of China). The assay kit for determining protein content was purchased from Biotech (USA).

Fullerenol and physicochemical characterization

Fullerenol powders were directly transferred to conducting resin.

Fullerenol morphology were observed by atomic force microscopy (SPM 3100, Veeco Instruments, Inc., U.S.A.) and scanning electron microscope (SEM, JSM-6700F, JEOL) at an acceleration voltage of 10 kV. The chemical properties of the fullerenol powder were characterized by elemental analysis (Flash EA 1112, ThermoFisher, USA), thermogravimetric analysis (Thermal gravimetric analyzer, Linseis, Germany) and ATR-FTIR spectroscopy (Nicolet iS 50 FT-IR, thermo, USA).

Animals

Male Wistar rats (6–7 weeks old) were purchased from the Hubei Province Experimental Animal Center (Wuhan, China) and housed in pathogen-free cages maintained at 24–26 °C, 55–75% humidity, and a 12-h light/dark cycle. The rats were fed a commercial diet (Hubei Province Experimental Animal Center) and given water ad libitum. All protocols used in these studies were approved by the Office of Scientific Research Management of Central China Normal University (November 8, 2011; CCNU-SKY-2012-011).

Primary hepatocytes from the rat liver

Wistar male rats were killed by cervical dislocation under general anesthetic. Livers were rapidly removed from the medical alcohol sanitized rats and placed in an ice-cold PBS solution and trimmed of adipose tissue. The livers were then finely minced and homogenized in ice-cold phosphate buffered saline (PBS buffer, pH=7.4). The cleaned liver organs were cut into pieces by ophthalmic scissors on a superclean bench. The whole process was performed on ice to maintain cell activity. Primary liver cell suspensions were obtained by filtering the tissue through medical gauze. The collected cells were dispersed by trypsinase treatment for 5min at 37°C. Cell culture mediums (DMEM/HIGH GLUCOSE, Hyclone) were then added to terminate trypsinization. Cell suspensions were centrifuged at 1000 rpm/min for 10 min at 4°C (low-temperature refrigerated centrifuge, Eppendorf 5417R). The supernatant was removed, and the collected cells were diluted by repeated pipetting to obtain a concentration of about 10^6 cells/mL. The viability of the prepared primary liver cells was calculated using the trypan blue exclusion test. Cell viability was determined to be over 95%.

Exposure to ethanol and fullerenol

Ethanol concentrations were prepared to 0.2, 2 and 20%. Fullerenol nanoparticles were dispersed in each ethanol group, with a concentration of 800µmol/l. The Fullerenol-Ethanol suspensions were sonicated for 5 minutes before use. 100 µl of primary liver cells (10^6 cells/mL) were mixed with each 100 µl of the prepared fullerenol-ethanol suspensions. Biomarker tests were carried out after 120 min incubation at 37°C with gentle shaking. The final ethanol concentrations in contact with the cells were 0.1, 1.0 and 10 %. The fullerenol concentration in cell contact was 400µmol/l. The ethanol

batches with concentrations of 0.1, 1.0 and 10 % were used as positive controls. The same amount of fullerenol in PBS and Vitamin C dissolved in 10% ethanol were also tested. Saline (0.9%) was used as the negative control.

Intracellular ROS measurement

Reactive oxygen species (ROS) were measured using oxidation-sensitive fluorescent DCFH-DA, which is a non-fluorescent compound that is freely taken up by cells and hydrolyzed by esterases to 2',7'-dichlorodihydrofluorescein (DCFH). DCFH is then oxidized to the fluorescent dichloro-fluorescein (DCF) in the presence of peroxides, thereby indicating the level of intracellular ROS. Briefly, cells were exposed to different concentrations as described in the section on exposure to ethanol and fullerenol. Then 100 µL of the tested suspension was transferred to a 96-well microplate, and 100 µL of DCFH-DA (10 µmol/L) was added. The reaction mixture was kept in the dark for 30 minutes at 37°C. The fluorescence intensity was measured at an excitation wavelength of 488 nm and an emission wavelength of 525 nm by a fluorescence reader (FLx 800; BioTek Instruments, Winooski, VT, USA)⁶⁵. Averages and standard deviations were based on five samples and all tests were performed in triplicate. Fluorescence images were captured by microscope (Nikon, Eclipse TS 100, Japan) after the liver cells attached onto the 96-well plates in a CO₂ incubator (Thermo Fisher, USA). The exposure procedures of material and dye were the same as described above.

GSH, MDA, 8-OHdG and TNF-α

Cells were exposed to different concentrations as described in the section on exposure to ethanol and fullerenol. All macromolecules to be examined were released from the liver cells through repeated freezing. Intracellular GSH and MDA content was measured following the kit manufacturers' instructions. The quantity of GSH and MDA in the samples or standards was calculated by absorbance measurement at OD405 and OD532. The concentrations of 8-OHdG and TNF-α were measured using ELISA kits according to manufacturer instructions. The pink or yellow-colored product formed is in proportion to the amount of TNF-α and 8-OH-dG respectively. Absorbance of the produced 8-OHdG and TNF-α was measured at OD450. The sensitivity of the TNF-α ELISA kit was 8 pg/mL. And the sensitivity of the 8-OH-dG ELISA kit was 0.5 ng/mL. Cell protein content was measured at OD562 using a BCA protein assay kit. Averages and standard deviations were based on five samples and all tests were performed in triplicate.

Biodistribution of fullerenol in rat metabolic organs

Fullerenol was delivered to the rat via tail intravenous injection after 2 hours and then again after 7 days. Wistar male rats were killed by cervical dislocation under general anesthesia. Organs (liver and kidney) were incubated in fixative (saturated 2,4,6-trinitrophenol/formalin/glacial acetic acid [15:5:1 v/v/v]) for 24 hours at room temperature. Hematoxylin and eosin (H&E)-stained slices were then prepared as Liu described⁶⁶. Stained pieces were embedded in paraffin, sectioned into 10 µm slices, and observed using a DM

4000B microscope (Leica, Berlin, Germany). The average optical density (OD) of each slice was determined using Image-Pro Plus 6.0 (Media Cybernetics, Bethesda, MD, USA) software. All tissue sections were examined qualitatively by two experienced pathologists in a blinded fashion.

Statistical analysis

GraphPad Prism software was used for statistical analysis of the experimental data, and for graphing the results. Results were evaluated statistically using an analysis of variance (ANOVA) followed by the Tukey test to determine the significance of the differences between groups. $p < 0.05$ is considered significant, $p < 0.01$ is considered a very significant difference and $p < 0.001$ is an extremely significant difference.

Conclusions

Hepatoprotective effects of fullerene nanoparticles in alcohol-induced oxidative stress were demonstrated in a rat liver primary hepatocyte. The fullerene nanoparticles in 400 $\mu\text{mol/L}$ exhibited excellent ROS scavenging ability. It effectively eliminated alcoholic oxidative damage and thus inhibited the alcohol-induced overexpression of TNF- α . Moreover, fullerene nanoparticles are easily absorbed by the liver and are excreted via the metabolic organs within a short period of time. Fullerene nanomaterials are potential biocompatible biomedical agents that could be used in preventive treatment of alcoholic hepatopathy.

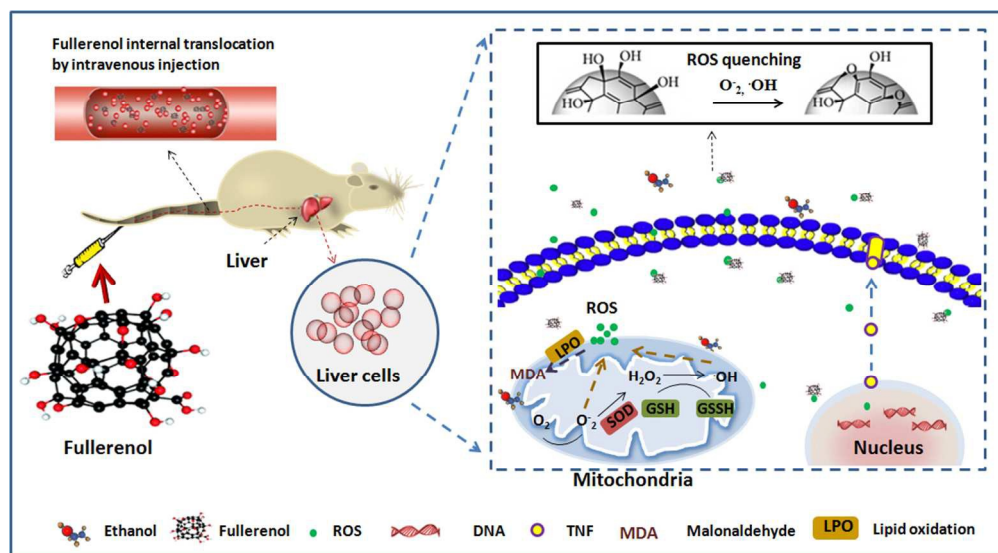
Acknowledgements

This work was supported by the Open Research Fund of the Key Laboratory of Sichuan Province of China (NJ2011-01), Talent Foundation of Sichuan University of Science & Engineering (2015RC13) and The Innovation and Entrepreneurship Students Training Project of Sichuan Province of China (201510622015).

References

1. F. Donato, A. Tagger, R. Chiesa, M. L. Ribero, V. Tomasoni, M. Fasola, U. Gelatti, G. Portera, P. Boffetta and G. Nardi, *Hepatology*, 1997, **26**, 579–584.
2. R. Baan, K. Straif, Y. Grosse, B. Secretan, F. El Ghissassi, V. Bouvard, A. Altieri, V. Coglianò and WHO International Agency for Research on Cancer Monograph Working Group, *Lancet. Oncol.*, 2007, **8**, 292–293.
3. The International Agency for Research on Cancer. GLOBOCAN 2012: estimated cancer incidence, mortality and prevalence worldwide in 2012. *World Health Organization*.
4. C. S. Lieber, *Alcohol*, 2004, **34**, 9–19.
5. A. G. Beckett, A. V. Livingstone and K. R. Hill, *BMJ*, 1961, **2**, 1113.
6. R. Bataller and D. A. Brenner, *J. Clin. Invest.*, 2005, **115**, 209.
7. T. A. Sofensen, K. Bentsen, K. Eghøj, M. Orholm, G. Højbye and P. Offersen, *The Lancet*, 1984, **324**, 241–244.
8. B. Sid, J. Verrax and P. B. Calderon, *Free. Radic. Res.*, 2013, **47**, 894–904.
9. Y. Yang, Z. Han, Y. Wang, L. Wang, S. Pan, S. Liang and S. Wang, *RSC. Adv*, 2015, **5**, 36732–36741.
10. D. F. Wu and A. I. Cederbaum, *Semin. Liver. Dis.*, 2009, **29**, 141–154.
11. A. Dey and A. I. Cederbaum, *Hepatology*, 2006, **43**, S63–S74.
12. A. I. Cederbaum, Y. Lu and D. Wu, *Arch. Toxicol.*, 2009, **83**, 519–548.
13. M. E. Medina, C. Iuga and J. R. Alvarez-Idaboy, *RSC. Adv.*, 2014, **4**, 52920–52932.
14. L. J. Marnett, *Mutat. Res.*, 1998, **424**, 83–95.
15. J. C. Fernández-Checa, N. Kaplowitz, C. García-Ruiz, A. Colell, M. Miranda, M. Marí, E. Ardite and A. Morales, *Am. J. Physiol.*, 1997, **273**, 7–17.
16. L. J. Hofseth and M. J. Wargovich, *J. Nutr.*, 2007, **137**, 183S–185S.
17. H. W. Kroto, J. R. Heath, S. C. O'Brien, R. F. Curl and R. E. Smalley, *Nature*, 1985, **318**, 162–163.
18. R. Bakry, R. M. Vallant, M. Najam-ul-Haq, M. Rainer, Z. Szabo, C.W. Huck, and G. K. Bonn, *Int. J. Nanomedicine*, 2007, **2**, 639–649.
19. R. S. Ruoff, D. S. Tse, R. Malhotra and D. C. Lorents, *J. Phys. Chem.*, 1993, **97**, 3379–3383.
20. G. Jia, H. Wang, L. Yan, X. Wang, R. Pei, T. Yan, and X. Guo, *Environ. Sci. Technol.*, 2005, **39**, 1378–1383.
21. K. Kokubo, S. Shirakawa, N. Kobayashi, H. Aoshima and T. Oshima, *Nano. Res.*, 2011, **4**, 204–215.
22. G. V. Andrievsky, V. I. Bruskov, A. A. Tykhomyrov, and S. V. Gudkov, *Free. Radic. Biol. Med.*, 2009, **47**, 786–93.
23. J. Mrdanovic, S. Solajic, C. Bogdanovic, K. Stankov, G. Bogdanovic and A. Djordjevic, *Mutat. Res.*, 2009, **680**, 25–30.
24. G. Bogdanovic, V. Kovic, A. Djordjevic, J. Kanadanovic-Brunet, M. Vojinovic-Milardov, V. V. Baltic, *Toxicol. In Vitro*, 2004, **18**, 629–637.
25. B. Srdjenovic, V. Milic-Torres, N. Grujic, K. Stankov, A. Djordjevic and V. Vasovic, *Toxicol. Mech. Methods*, 2010, **20**, 298–305.
26. X. Yang, C. J. Li, Y. Wan, P. Smith, G. Shang and Q. Cui, *Int. J. Nanomedicine*, 2014, **9**, 4023–4031.
27. S. M. Mirkov, A. N. Djordjevic, N. L. Andric, S. A. Andric, T. S. Kostic, G. M. Bogdanovic and R. Z. Kovacevic, *Nitric Oxide*, 2004, **11**, 201–207.
28. R. Injac, M. Perse, N. Obermajer, V. Djordjevic-Milic, M. Prijatelj, A. Djordjevic and B. Strukelj, *Biomaterials*, 2008, **29**, 3451–3460.
29. W. H. Yang, D. B. Chen and X. M. Wang, *PPS*, 2004, **28**, 243–246.
30. B. Srdjenovic, V. Milic-Torres, N. Grujic, K. Stankov, A. Djordjevic and V. Vasovic, *Toxicol. Mech. Metho.*, 2010, **20**, 298–305.
31. J. Y. Xu, Y. Y. Su, J. S. Cheng, S. X. Li, R. Liu, W. X. Li and Q. N. Li, *Carbon*, 2010, **48**, 1388–1396.

32. K. Tanaka, M. Sato, Y. Tomita and A. Ichihara, *J. Biochem.*, 1978, **84**, 937-946.
33. W. X. Ding, H. M. Shen, H. G. Zhu and C. N. Ong, *Environ. Res.*, 1998, **78**, 12-18.
34. T. S. Naimi, D. E. Nelson and R. D. Brewer, *Am. J. Prev. Med.*, 2010, **38**, 201-207.
35. N. Wang, L. Sun, X. Zhang, X. Bao, W. Zheng and R. Yang, *RSC Adv.*, 2014, **4**, 25886-25891.
36. V. C. Sanchez, A. Jachak, R. H. Hurt and A. B. Kane, *Chem. Res. Toxicol.*, 2011, **25**, 15-34.
37. K. Kobayashi, H. Ueno, K. Kokubo, M. Yudasaka and H. Yasuda, *Carbon.*, 2014, **68**, 346-351.
38. Z. Marković and V. Trajković, *Biomaterials.*, 2008, **29**, 3561-3573.
39. J. B. Hoek and J. G. Pastorino, *Alcohol.*, 2002, **27**, 63-68.
40. J. Safaei-Ghomi and R. Masoomi, *RSC Adv.*, 2014, **4**, 2954-2960.
41. R. Injac, M. Perse, N. Obermajer, V. Djordjevic-Milic, M. Prijatelj, A. Djordjevic and B. Strukelj, *Biomaterials.*, 2008, **29**, 3451-3460.
42. I. Rade, G. Biljana, D. Aleksandar and S. Borut, *Afr. J. Biotechnol.*, 2008, **7**(25).
43. A. Djordjevic, B. Srdjenovic, M. Seke, D. Petrovic, R. Injac and J. Mrdjanovic, *J. Nanomater.*, 2015, **2015**, 1-15.
44. A. Djordjevic, J. M. Canadanovic-Brunet, M. Vojinovic-Miloradov, and G. Bogdanovic, *Oxid. Comm.*, 2004, **27**, 806-812.
45. R. Nordmann, C. A. T. H. E. R. I. N. E. Ribire and H. Rouach, *Alcohol. Alcoholism.*, 1990, **25**, 231-237.
46. J. Li, L. Li, X. Liu, R. Li and X. Yang, *RSC Adv.*, 2013, **3**, 25388-25395.
47. J. B. Schulz, J. Lindenau, J. Seyfried and J. Dichgans, *Eur. J. Biochem.*, 2000, **267**, 4904-4911.
48. B. Halliwell and S. Chirico, *AJCN.*, 1993, **57**, 715S-724S.
49. R. Polavarapu, D. R. Spitz, J. E. Sim, M. H. Follansbee, L. W. Oberley, A. Rahemtulla and A. A. Nanji, *Hepatology.*, 1998, **27**, 1317-1323.
50. R. Anderson and A. R. Barron, *JACS.*, 2005, **127**, 10458-10459.
51. J. E. Klaunig, L. M. Kamendulis and B. A. Hocevar, *Toxicol. Pathol.*, 2010, **38**, 96-109.
52. R. F. Schwabe and D. A. Brenner, *Am. J. Physiol-Gastr. L.*, 2006, **290**, G583-G589.
53. L. Xu, Y. Wei, D. Dong, L. Yin, Y. Qi, X. Han and J. Peng, *RSC Adv.*, 2014, **4**, 30704-30711.
54. X. Zhang, X. Han, L. Yin, L. Xu, Y. Qi, Y. Xu and J. Peng, *Sci. Rep-UK.*, 2015, **5**.
55. F. Balkwill, *Cancer. Metast. Rev.*, 2006, **25**, 409-416.
56. H. Walczak, *Immunol. Rev.*, 2011, **244**, 9-28.
57. B. A. Holm, E. J. Bergey, T. De, D. J. Rodman, R. Kapoor, L. Levy and P. N. Prasad, *Mol. Cryst. Liq. Cryst.*, 2002, **374**, 589-598.
58. J. P. M. Almeida, A. L. Chen, A. Foster and R. Drezek, *Nanomedicine.*, 2011, **6**, 815-835.
59. J. Grebowski, P. Kazmierska and A. Krokosz, *Biomed. Res. Int.*, 2013, **2013**, 1-9.
60. Z. Q. Ji, H. Sun, H. Wang, Q. Xie, Y. Liu and Z. Wang, *JNR.*, 2006, **8**, 53-63.
61. R. Injac, N. Radic, B. Govedarica, M. Perse, A. Cerar, *Pharmacol. Rep.*, 2009, **61**, 335-342.
62. S. Trajković, S. Dobrić, V. Jačević, V. Dragojević-Simić, Z. Milovanović and A. Đorđević, *Colloids. Surf. B. Biointerfaces.*, 2007, **58**, 39-43.
63. R. Kubota, M. Tahara, K. Shimizu, N. Sugimoto, A. Hirose and T. Nishimura, *Toxicol. Lett.*, 2011, **206**, 172-177.
64. J. Y. Xu, Y. Y. Su, J. S. Cheng, S. X. Li, R. Liu, W. X. Li and Q. N. Li, *Carbon.*, 2010, **48**, 1388-1396.
65. D. Wu, J. Lu and Y. Zhang, *Toxicol. Appl. Pharmacol.*, 2013, **271**, 127-136.
66. X. Liu, Y. Zhang, J. Li, D. Wang, Y. Wu, Y. Li and X. Yang, *Int. J. Nanomedicine.*, 2014, **11**, 823-839.



300x164mm (96 x 96 DPI)